Verification within wave resource assessments. Part 2: Systematic trends in the fit of spectral values

Verification within Wave Resource Assessments. Part 2: Systematic Trends in the Fit of Spectral Values

EC Edwards[1], LC Cradden[1], DM Ingram[1], C Kalogeri[2]

[1]Institute for Energy Systems, University of Edinburgh, Edinburgh EH9 3JL
[2]Atmopsheric Modelling and Forecasting Group, National Kapodistrian University of Athens, Greece

Key Words: wave energy, wave power, resource assessment, spectral analysis, model validation, WAM, EMEC test site, numerical model

ABSTRACT

Interest in wave energy as a viable renewable energy has increased greatly in the past couple of decades. To determine the potential that a certain location has to harvest wave energy, a resource assessment must be performed for that location. As wave energy converter technologies get closer to market, it is becoming necessary to undertake more detailed resource assessments to determine the optimal location for deployment as well as the design and operating sea states. This study shows the level of sophistication that must be included in the verification process within a wave resource assessment. We describe the methodology in two articles. Part 1 described a procedure for a complete statistical analysis of the fit of the model. This paper will demonstrate how investigating systematic trends in the fit of spectral values is essential for determining the precise problem areas of the model and is thus required as part of the verification processes. Lacking this detail could mean failing to notice potentially vital issues for energy extraction at the location of interest. The identification of specific problem areas will enable a well-informed consideration of the necessary next steps for improved prediction of energy extraction.

1. Introduction

Part 1 revealed why it is important within a resource assessment to do a thorough statistical analysis of relevant parameters. Specifically, significant wave height and energy period calculations from the WAM3 CY331 model [1, 2, 3] were compared with corresponding measurements from a nearby Waverider buoy. Part 2 will demonstrate that it is also important to look beyond the parameters into the raw sea states by comparing spectra from the buoy and model. Comparing spectra will give a better understanding of the fit of the model at the location of interest. While comparing spectra is commonplace in many validation studies done by wave modellers, there are currently no resource assessments that quantitatively compare systematic problems in spectra for the model against *in situ* measurements. This analysis is essential for determining any subsequent steps that need to take place in a resource assessment to improve the reliability of predictions of resources.

In the introduction for Part 1, verifications or validation sections within global, national, and local resource assessments were reviewed. Within the studies

mentioned, none of the global or national resource assessments revealed any spectral analysis. Within the local resource assessments, there were a few mentions of studying spectra, but no systematic analyses were done. Liberti et al. [4] examined the mean wave direction, and calculated circular statistics for bias and variance. Van Nieuwkoope et al. [5] compared one-dimensional spectra for sites within the resource assessment, but this comparison was not done for the purpose of verification and there was no comparison to *in situ* measurements.

Wave models themselves are very well validated individually, and there have been an extensive number of very thorough studies describing validations of different wave models [e.g. 6, 7, 8, 9, 10, 11]. When doing a resource assessment, it is necessary to go into a similar amount of detail as these validations provide the necessary specific and accurate predictions for the energy sector. The WISE Group [12] produced a recent report on the current state of oceanographic wave modelling. Within this report, there is a section on the inevitable limitations of wave models and a description of different types of errors that can occur in models. These include errors due to resolution (geographic and spectral), diffusion, and dispersion, and many more types of errors. This paper indicates that although oceanographic wave models perform well overall, there are known areas of the models for which results need to be taken with caution. It is necessary to see if any of these problems occur at the location of interest for a resource assessment to determine the impact of the problems on the predictions, and finally to resolve further steps which need to be taken to improve the predictions

Krogstad et al. [13] has a section on inter-comparisons of wave parameter measurements. Within this section, there is a description of a comparison of frequency spectra as well as a comparison of directional spectra. Demonstrating the high level of detail within this study, to compare the frequency spectra a plot was made of mean spectral ratio over fixed frequencies, and to compare directional spectra particular cases were presented by comparing the buoy results to the radar used. The aforementioned validation studies of wave models show varying amounts of detail, but most looked within the spectra at least to point out particular case studies.

Mackay et al. [14] concentrates on the Measure-Correlate-Predict (MCP) method of predicting an energy yield and shows how to find uncertainty bounds on the estimate. This is a very powerful method, but if the goal of a resource assessment is to understand the fit of the model to the location of interest with more detail, or to try to make the data more accurate, this method may not be appropriate.

These studies (Cavaleri, Krogstad, and Mackay) show the high level of detail within validations done by wave modellers. The purpose of Part 2 is to demonstrate the increasing importance of a high level of detail of verifications within resource assessments by comparing spectra. It is shown that the specific problems within the model used by this study at the location of interest occur within low-frequency waves coming from the West that are acting as intermediate-depth waves. These results give a further understanding of the fit of the model at the location off the

Orkney Islands and insight into the next steps that need to be taken to improve the accuracy of the data for predicting wave power potential. Specifically, the fundamental next step in this analysis would be to use a coastal model, such as SWAN, to account for shallow water physics.

Section 2 will show methodology and results. First, background of the wave model used and the buoy data will be introduced (section 2.1). Then, the specific records at which the model and buoy values most dramatically differ are examined in detail (section 2.2). Next, we compare values within each spectral bin to determine any overall trends (section 2.3). Finally, we investigate the problem areas in connection with the dispersion relation (section 2.4). Section 3 summarizes the findings of this paper, connects the analysis with Part 1, and discusses potential further work to be carried out on the subject, specifically showing that a shallow-water model, such as SWAN, should be used.

2. Methodology and Results

2.1 Background

This study compares results from a wave model to *in situ* observations from a buoy. The wave system used for this analysis is the ECMWF Cy331 version [2, 16] of WAve Model (WAM) [17, 18]. The model solves the spectral action balance equation without any presumptions on the shape of the wave spectrum and represents the physics of the evolution of the wave spectrum in accordance with our current knowledge using the full set of degrees of freedom of a two-dimensional wave spectrum. The grid resolution can be arbitrary in space and time. The propagation can be done on a latitudinal – longitudinal or on a Cartesian grid. WAM is able to run in a deep-water or a shallow-water mode and includes the effect of wave refraction caused by changes in depth and by ocean currents.

This particular version, developed at the National Kapodistrian University of Athens (NKUA), incorporates a number of important implementations that increase the potential capabilities of the wave system. Some of the most important improvements include the new advection scheme, which takes corner points into account, and thus provides a more uniform propagation in all directions, using the new Corner Transport Upstream scheme [19], and the new parameterization of the shallow water effects. In particular, in shallow water the four-wave interaction is vanished by the wave induced currents generated by the finite amplitude surface gravity waves. Thus following the work of Janssen and Onorato, [20], a parameterization of this shallow water effects is introduced and affects both the evolution of the wave spectra and the determination of the kurtosis of the wave field.

The wave model has been configured to run in computational domain covering the North Atlantic between latitudes 20°N and 75°N and longitudes 50°W and 30°E. The domain extends far beyond the area of interest aiming to capture the important

swell propagation. It is discretized in a considerably high resolution of (0.05 x 0.05 degrees) which has been adopted as suitable for capturing the fine-scale features in a credible way. The wave spectrum has been discretized in 25 frequencies (logarithmically spaced from 0.0417 to 0.5476 Hz) and 24 equally spaced directions. A 75-second time-step was selected so as to satisfy the CFL stability criterion. The wave model operated was driven by 3-hourly 10m winds provided by the regional atmospheric modelling system SKIRON [21, 22]. The horizontal resolution of the SKIRON model is also 0.05 x 0.05 degrees extending from surface up to 50hPa in 45 vertical levels using a 15-sec time-step. The wave model provides outputs for wide range of wave parameters and components such as wave height (significant and swell), directions, energy and peak period. The result is full wave spectrum at preselected grid points.

Information was extracted from 12 of the model's grid points, which were located near the European Marine Energy Centre (EMEC) wave test site off the coast of the Orkney Islands, Scotland. The buoy is a Datawell Waverider Buoy situated at the EMEC wave test site (58.98˚N, 3.39˚W) [3]. Hourly buoy data was available from 1/1/2006 to 26/12/2007, with 674 records missing (3.8% of total). While the analysis in Part 1 focused on the wave parameters significant wave height (H_{m0}) and energy period (T_e), this paper compares hourly spectral outputs from the model to corresponding data from the buoy. The model outputs are from grid point 7 (see Figure 1 of Part 1).

Part 1 showed the importance of comparing spatial and temporal scales of the data, but it is additionally important to compare spectral scales, for both directions and frequencies. As detailed above, the model outputs full two-dimensional directional spectra, but the directionality in the buoy is only represented by mean and spread. To make directional bins comparable it is necessary to interpolate the information given by the buoy using a directional spread function. This spreading function, represented by a wrapped normal function, is defined by

$$D(f,\theta) = \frac{\exp\left[-\frac{1}{2}\left(\frac{\theta-\theta_0}{\sigma}\right)\right]}{\sqrt{2\pi}\sigma} \tag{5}$$

Where σ = the directional spreading parameter, and θ_0 is the mean wave direction. Then, the full directional spectrum is found by

$$E(f,\theta) = E(f)D(f,\theta) \tag{6}$$

Where $E(f)$ is the energy spectral density function [15]. For each frequency and direction, $E(f,\theta)$ is calculated for the buoy using the maximum PSD times the normalized PSD multiplied by $D(f,\theta)$, using the mean direction and directional spread for that particular frequency. Frequency ranges differ between buoy and model spectral files as described above (buoy: 0.055 Hz to 0.4924 Hz, model: 0.0225 to 0.585 Hz) [23, 2].

2.2 Problem areas

The final step within the statistical analyses described in Part 1 was to construct and analyze statistical models for H_{m0} and T_e to describe the fit of the model values to corresponding buoy vales. Specifically, a generalized linear model was chosen for H_{m0} and a linear model was chosen for T_e. This analysis showed data points which were particularly influential on the statistical model. For H_{m0}, these points correspond to 23 February 2006 11:00, 26 September 2006 9:00, and 27 Sep 2006 11:00. For T_e, these points are 23 February 2006 11:00, 6 April 2006 14:00, and 26 September 2006 12:00.

Each of the problematic data points was studied individually. First, the context of the records was considered. Two hours before and two hours after were examined. Data from the buoy for half-past the hour was also available, so this was also included. Because 23 February 2006 11:00 was on both lists, it is shown in Table 1.

Table 1: Records from 23 February 2006 including time, values from the Waverider Buoy and WAM CY331 wave model for significant wave height (H_{m0}) in meters and energy period (T_e) in seconds

Time	Buoy H_{m0}	Model H_{m0}	Buoy T_e	Model T_e
9:00	1.7	2.0	9.6	13
9:30	1.7		9.9	
10:00	1.6	1.9	9.8	12
10:30	1.5		8.9	
11:00	10	1.8	25	12
11:30	1.8		9.9	
12:00	1.9	1.8	9.8	12
12:30	1.8		9.9	
13:00	1.8	1.7	9.9	12
13:30	1.8		9.7	

Table 1 shows that, for both H_{m0} and T_e, the collocations before and after 11:00 are very similar. At 11:00, the buoy values drastically differ from its surrounding values. This suggests that it is the output from the buoy that is unreliable at this time record. 6 April 2006 14:00 and 9 January 2007 10:00 showed similar behaviour, and it was determined that the data is unreliable at these times as well. For 26 September 2006 12:00, the model and buoy were close together for both 10:00 and 11:00, and then after 12:00 the buoy did not record values for the next 21 hours. This suggests that the buoy went out of service for a period, and it is sensible not to rely on the buoy value right before this “out-of-service” time period. These findings show how important data quality is and how important it is to do quality checks before doing a resource assessment with buoy data. Context of data must be examined before pre-emptively jumping to any conclusions about the performance of the model. A recommended standard for quality control of data can be seen in [24].

After examining each influential point, an entire time period was examined, during which the model and buoy values differed significantly and consistently. The problematic time period was observed from the time series plots in Part 1, reproduced here (Figure 1). The problematic time period is from 9 December to 17 December, 2006.

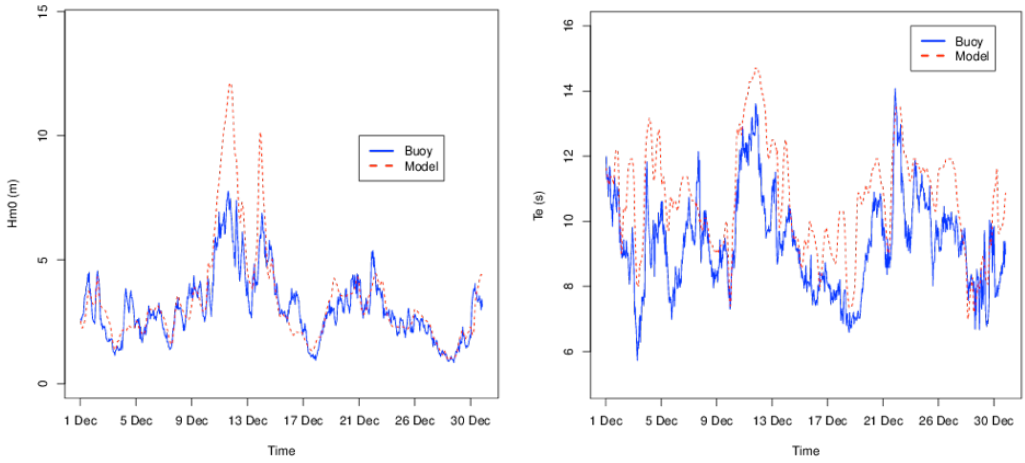

Figure 1: Time series of hourly H_{m0} and T_e (left and right, respectively) values from the wave model and the buoy from 1 December 2006 to 31 December 2006

During this time period the model over-exaggerates trends in significant wave height and energy period. The spectra of records during this time period were examined to further investigate the problem areas of the model. A full, two-dimensional spectrum was constructed for the buoy through the directional spreading function mentioned in section 2.1. Then, the Matlab package DIWASP (DIrectional WAve SPectra Toolbox) [25] was used to visually represent the spectra. This was done for buoy and model separately to perform a side-by-side comparison for each time record during the time period. Figures 2 and 3 show an example: Figure 2 shows the spectra for the model for 12 December 2006 8:00, and Figure 3 shows the corresponding spectrum for the buoy.

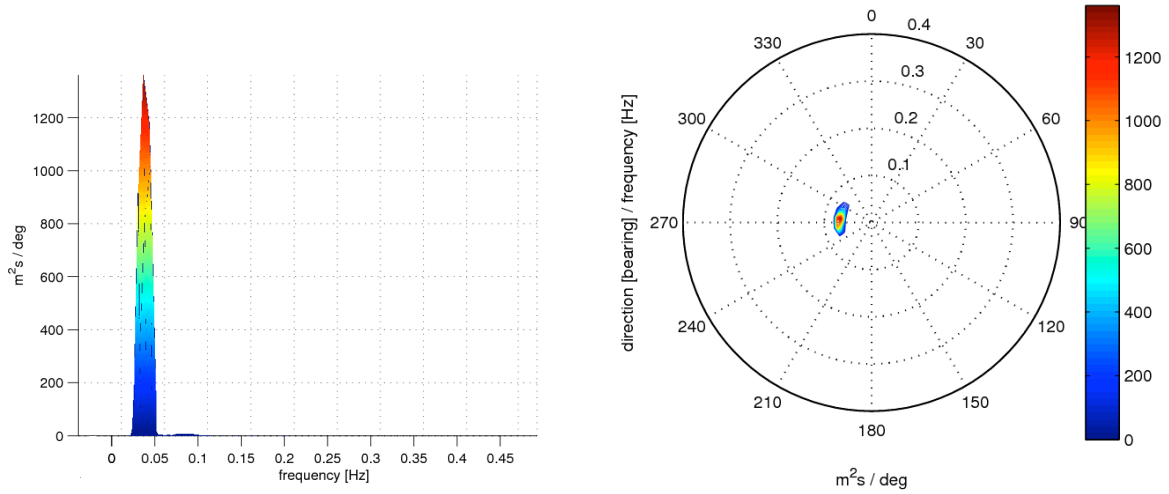

Figure 2: 12 December 2006 8:00 spectra for the wave model: Left: spectra collapsed into one dimension to show the peak (specific energy vs. frequency, directionality ignored); Right: 2D plot showing direction (angle from 0), frequency (radial distance from origin), and specific energy magnitude (colour). Note that the colour scale extends to approximately 1300 m^2s/ deg.

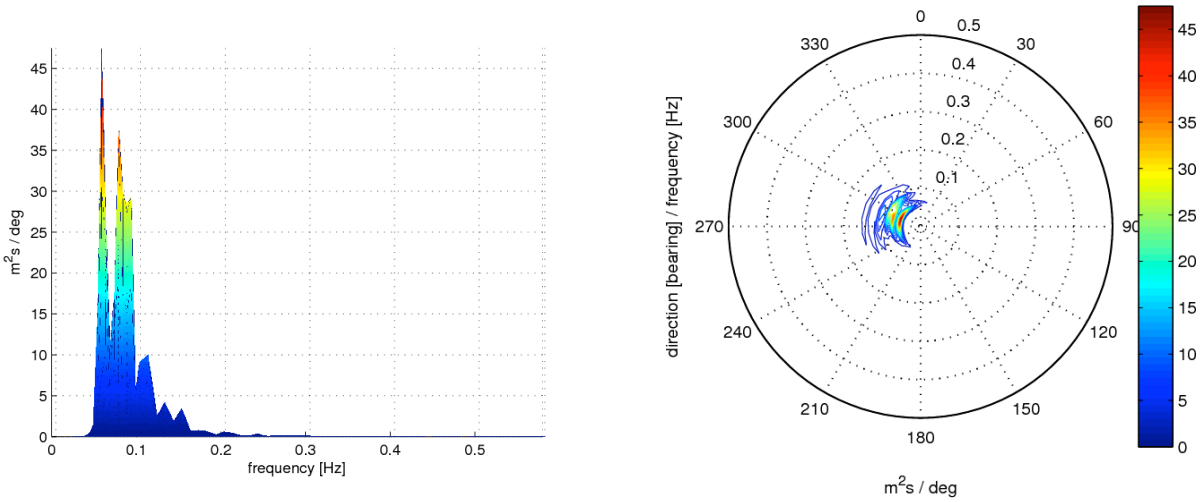

Figure 3: 12 December 2006 8:00 spectra for the buoy: Left: spectra collapsed into one dimension to show the peak (specific energy vs. frequency, directionality ignored); Right: 2D plot showing direction (angle from 0), frequency (radial distance from origin), and specific energy magnitude (colour). Note that the colour scale extend to approximately 47 m^2s/ deg.

Figures 2 and 3 show the 2-dimensional spectra in two different ways for the model and the buoy, respectively. The most important part of these figures to notice is the scale of the specific energy: the scale for the model extends to approximately 1300 m^2s/deg, whereas the scale for the buoy only extends to approximately 47 m^2s/deg. This demonstrates that the model is over-estimating the specific energy. We see from the polar-type plots (on the right in both figures) that the model is predicting

that all of the energy is coming from the West, but the buoy has a larger spread with the most energy coming from slightly North of West. We also see from the surface-type plots (on the left in both figures) that the model predicts that all of the energy is coming from very small frequencies (0.025 to 0.05), whereas the buoy records a wider spread of frequencies. In summary, we have determined that the model over-estimates the energy in low-frequency waves coming from the West. The next step is to see if this problem is universal.

2.3 Spectral analysis

To determine if the model generally over-predicts energy from low-frequencies from the West, or if it is only during the time period examined (9 Dec to 17 Dec 2006), the spectra from the model and buoy must be compared at each time record. The first step in this comparison of the two spectra was to compare the directional component. Within each spectrum, the specific energy was summed over all frequencies for each direction. Since the model and buoy spectra are both represented by the same 24 directions, a direct comparison is appropriate. To represent the comparison, the absolute value of the error between specific energy (summed over frequency) of buoy and model is plotted against the corresponding direction. This is done for each direction and each time record, for a total of 420,480 pairs of records, shown in Figure 4.

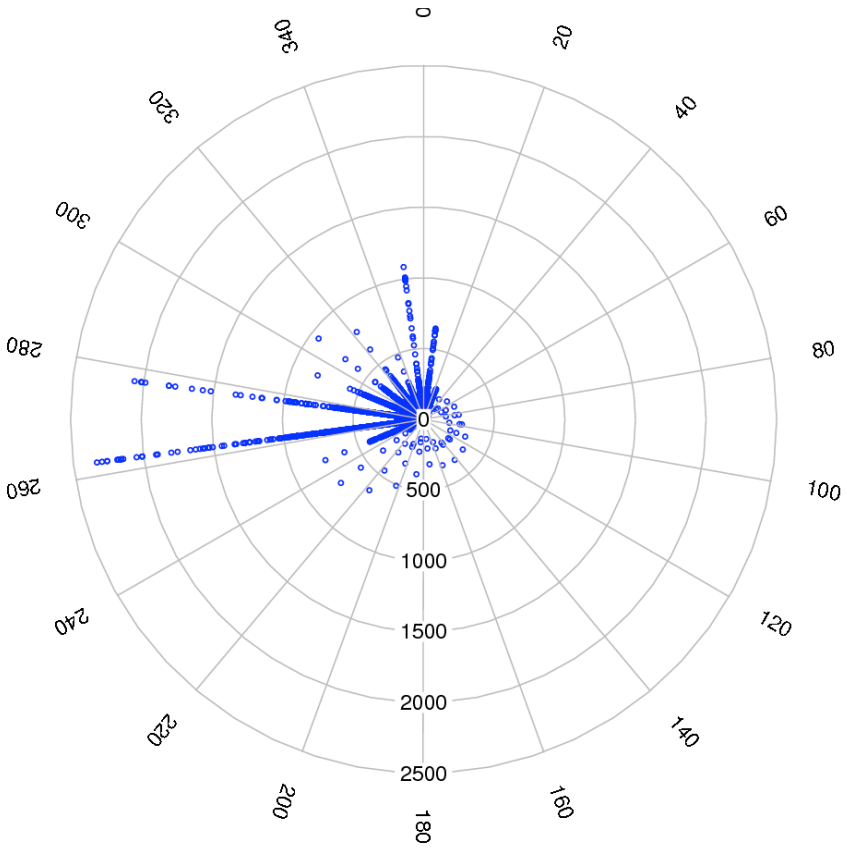

Figure 4: The absolute value of the error between buoy and model of specific energy summed over frequency (m^2s/deg) for each direction and each time record plotted against direction (degree) [26]

Figure 4 shows that the largest errors occur within the Western bins (262.5° and 277.5°). This clearly reveals where the largest errors are, but to see if these directional bins are problematic universally, the mean and median of the absolute value errors for each direction were plotted against direction, as seen in Figure 5.

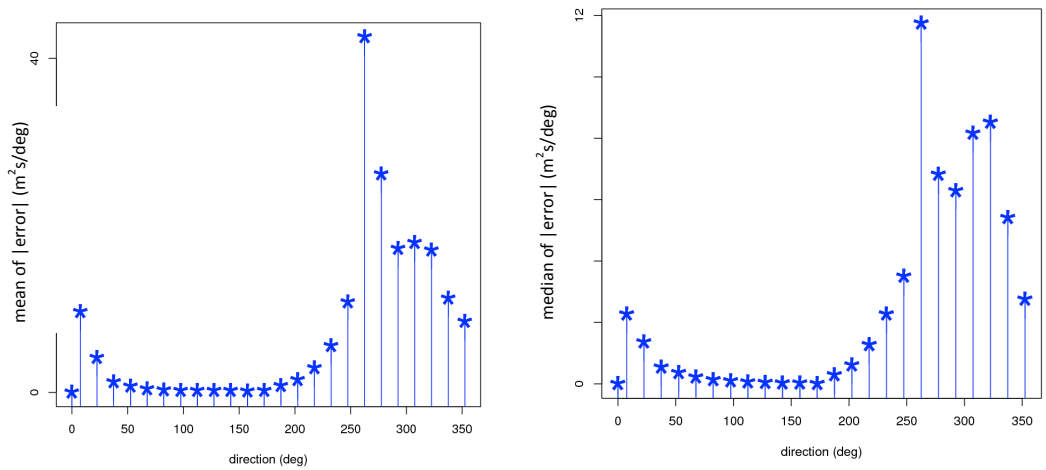

Figure 5: The mean (left) and median (right) of the errors of specific energy summed over frequency (m^2s/deg) within each directional bin against direction

Figure 5 shows that the means are also largest in the Western bins (262.5° and 277.5°) and that the median is largest in the 262.5° bin. Figures 4 and 5 reveal that the model performs poorly at predicting waves from the West. Specifically, it over-predicts waves from this direction. This is particularly problematic at EMEC since Atlantic swell comes predominantly from the West.

Next, the frequency component of the spectra must be compared between buoy and model. As mentioned in section 2.1, the frequency ranges and the size of the frequency bins differ. So, a process of geometrical summation was necessary so as to not lose or gain any false specific energy. Both spectra were re-binned into spectra of 49 frequencies and 24 directions. The frequency bins vary in size, ranging from 0.0225 to 0.585 Hz. 49 frequencies were chosen because they best represent the combinations of bins from both spectra. It is important to remember that the frequencies in the original buoy spectral files range from 0.0225 to 0.585 Hz, whereas the frequencies in the original model spectral files range from 0.055 to 0.4924 Hz. Similar to direction, the error in specific energy summed over direction between buoy and model was found for each frequency for each time record. This resulted in 585,480 pairs of records. The errors were plotted against corresponding frequency, as shown in Figure 6.

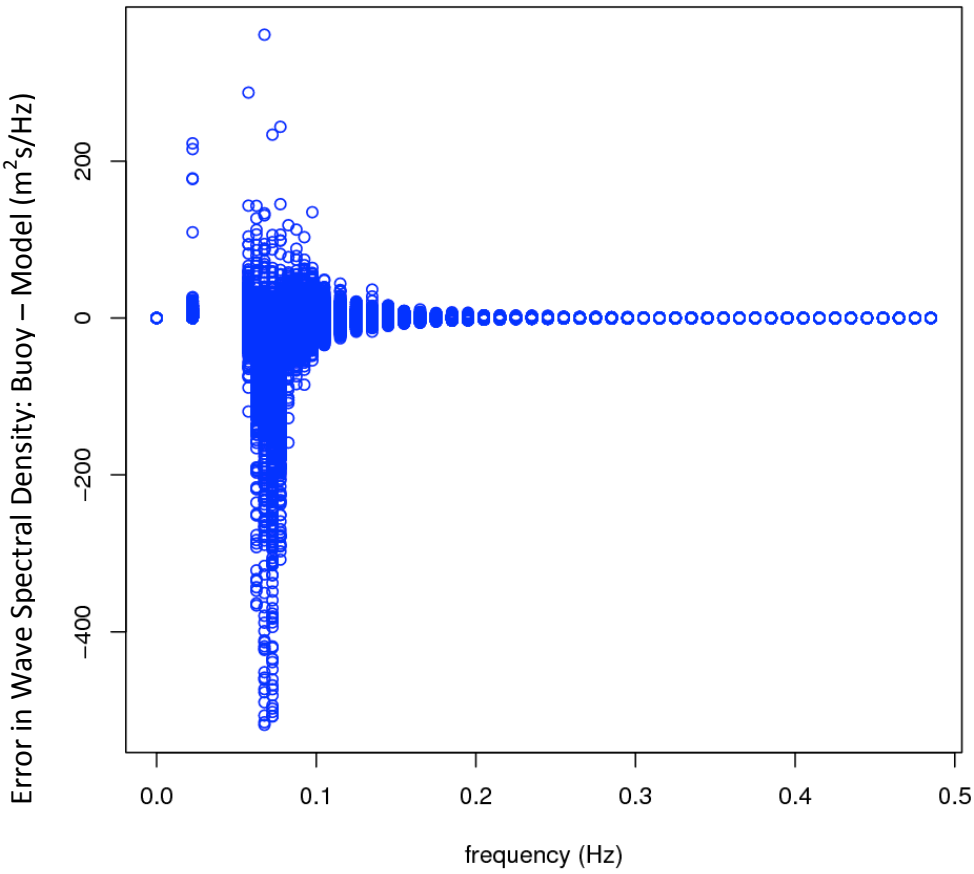

Figure 6: The error between buoy and model of specific energy summed over direction (m^2s/Hz) for each frequency and each time record plotted against frequency (Hz)

Figure 6 shows that the largest errors occur in frequencies between 0.05 Hz and 0.1 Hz. To examine if the typical errors occur within these frequencies, the mean and absolute value errors for each frequency were plotted against the corresponding frequency, as seen in Figure 7.

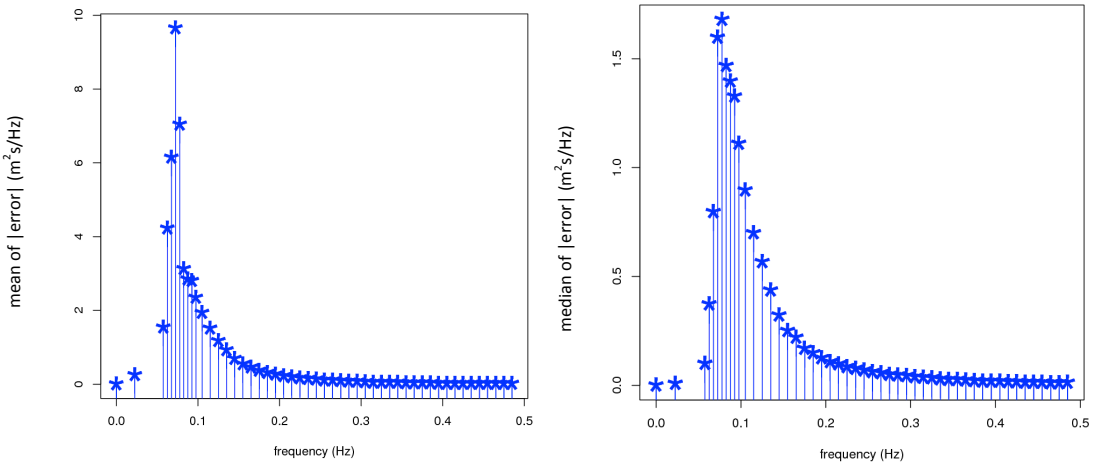

Figure 7: The mean (LEFT) and median (RIGHT) of the errors of specific energy summed over direction (m^2s/Hz) within each frequency bin against corresponding frequency

Figure 7 shows that the highest mean and median errors do occur in frequencies between 0.05 to 0.1 Hz. The next step is to determine if the two observed problems—Western bins and low frequencies—occur at the same time. We wish to determine if the problem records seen in Figures 4 and 5 occur simultaneously with the problem records seen in Figures 6 and 7. To do this, the error within each (re-binned) spectral bin is examined. The mean within each bin is examined to see where the "typical" errors are occurring, and the 99^{th} percentile within each bin is examined to see where the largest problems are occurring. These can be seen in Figures 8 and 9, respectively.

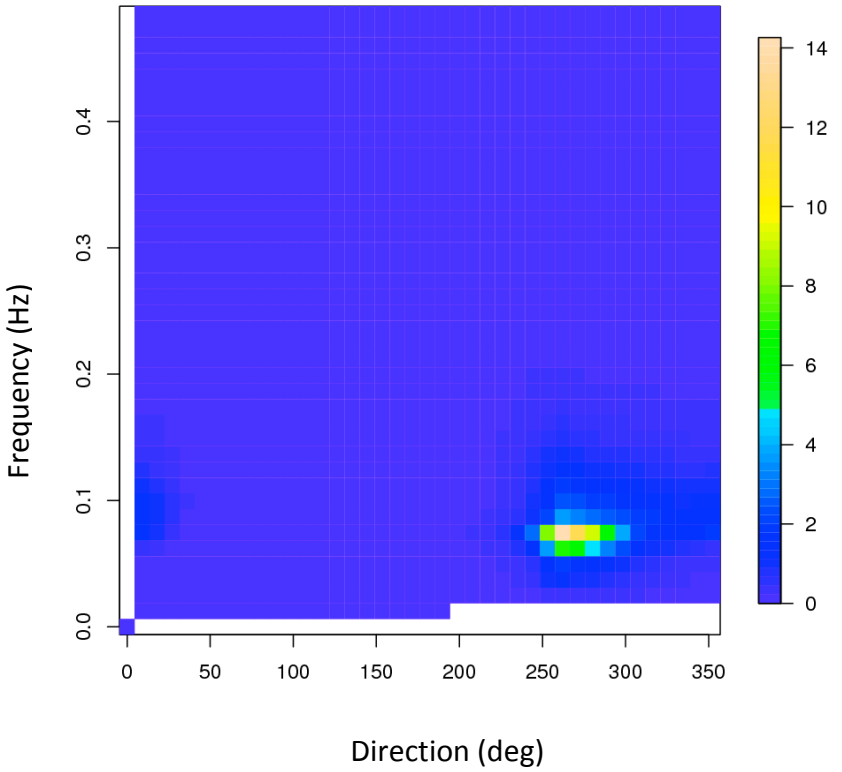

Figure 8: x-axis: direction (deg); y-axis: frequency (Hz); colour scale: mean of the absolute value of error between buoy and model within each (re-binned) spectral bin (m^2s/Hz-deg) [27, 28]

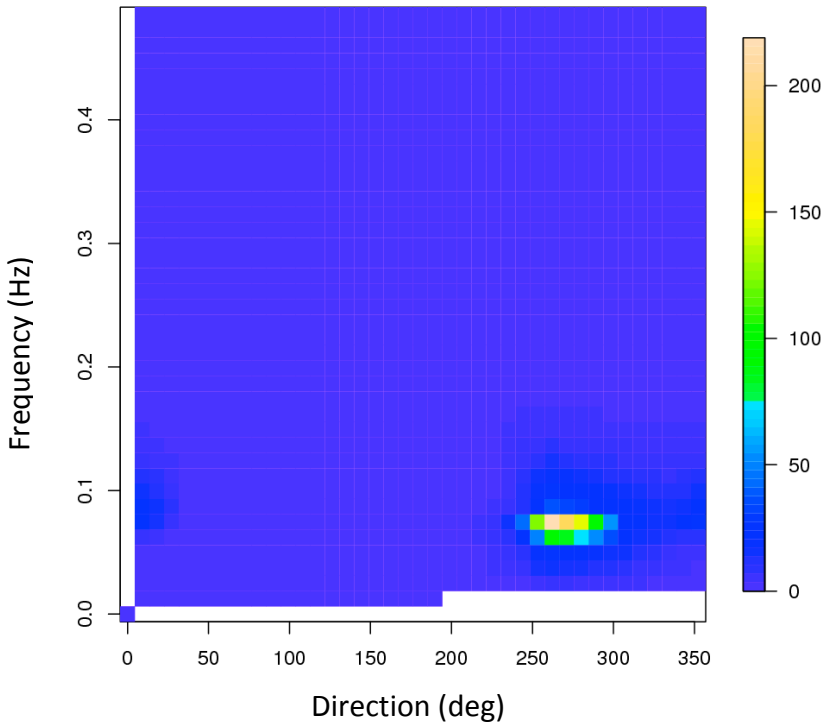

Figure 9: x-axis: direction (ɑegɹ; y-axıs: ɪrequency (Hz); colour scale: 99th of the absolute value of error between buoy and model within each (re-binned) spectral bin (m^2s/Hz-deg) [27, 38]

It can be determined from Figures 8 and 9 that both "typical" problems as well as the largest problem areas are from low-frequency waves coming from the West. To investigate this further, this observation is looked at in the context of the dispersion relation.

2.4 Dispersion relation

Following from linear wave theory, the dispersion relation is described by

$$\omega^2 = gk \tanh kh \tag{1}$$

where ω is the angular frequency, g is the acceleration of gravity, k is the wave number, and h is the water depth. Inserting the relations

$$\omega = \frac{2\pi}{T}, \tag{2}$$

$$k = \frac{2\pi}{\lambda}, \tag{3}$$

And

$$f = \frac{1}{T} \tag{4}$$

Into equation (1), where T is wave period, λ is wavelength, and f is frequency, and solving for f [29], results in

$$f = \frac{\pm\sqrt{\frac{2\pi g}{\lambda}\tanh\left(\frac{2\pi h}{\lambda}\right)}}{2\pi} \tag{5}$$

Water waves are divided into three different categories—shallow, intermediate, and deep—according to their relative depth h/λ, where h is the water depth. According to Rahman [29], if h/λ<1/20 the wave is said to be shallow, if h/λ>1/2 the wave is said to be deep, and otherwise the wave is considered intermediate.

To determine the range of frequencies that would qualify as shallow, intermediate, and deep, it is necessary to define the corresponding wavelengths.

Shallow: $\lambda > 20h$
Deep: $\lambda < 2h$
Intermediate: $20h < \lambda < 2h$

Since the model's input water depth at the point of interest (approximately 55 meters) is different to the buoy's measured water depth (52 meters), these calculations must be done separately.

For both buoy and model, corresponding values of h and λ are put into equation (5) to determine cut-off frequencies for "shallow" and "deep" waves. Then, these cut-off frequency values were examined in the context of Figure 6 (error within frequency bins).

Buoy:

Table 2: Wavelengths and corresponding frequencies at which waves change from shallow to intermediate and from intermediate to deep for the Waverider Buoy, which records the depth as 52 meters

	Deep	Shallow
λ	< 104 m	> 1040 m
f	> 0.1223 Hz	< 0.0214 Hz

Model:

Table 3: Wavelengths and corresponding frequencies at which waves change from shallow to intermediate and from intermediate to deep for the wave model at grid point 7, which inputs a water depth of 55 meters

	Deep	Shallow
λ	< 110 m	> 1100 m
f	> 0.1189 Hz	< 0.0208 Hz

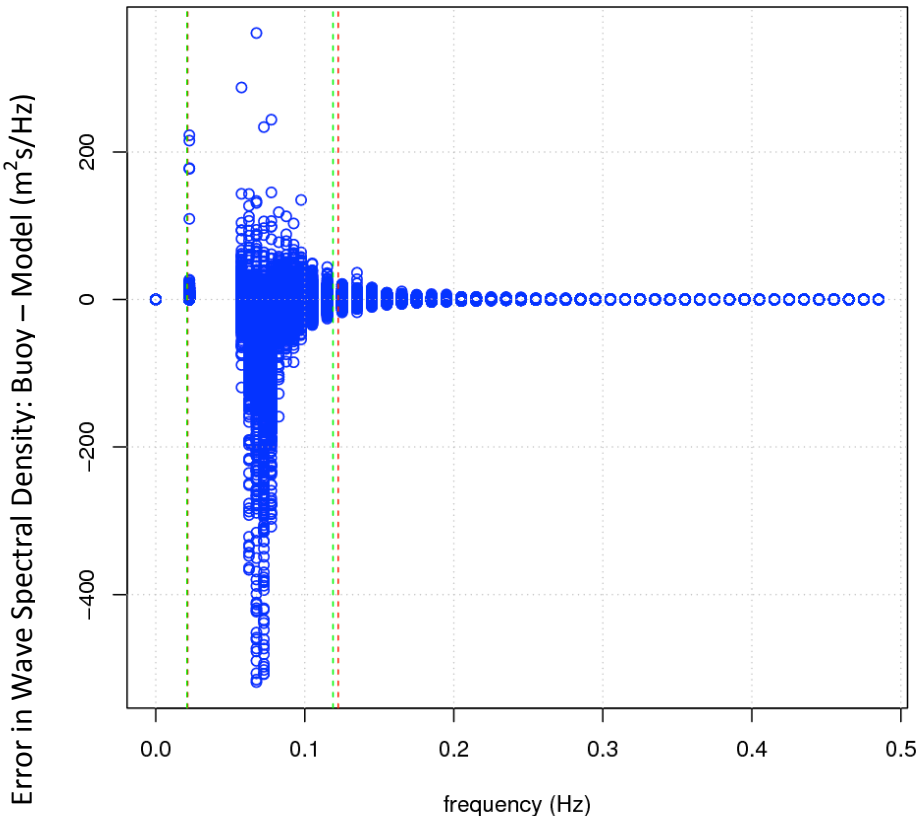

Figure 10: The error between buoy and model of specific energy summed over direction (m^2s/Hz) for each frequency and each time record plotted against frequency (Hz) with lines representing cut-off frequencies at which waves switch from shallow to intermediate (left lines) and intermediate to deep (right lines) for buoy (red) and model (green)

It is determined from Figure 10 that the problems in the model are occurring from intermediate waves.

3. Discussion and Conclusion

The need for spectral analysis in verification processes within resource assessments has been demonstrated. As an illustrative case study, the performance of the wave model WAM3 CY331 at a location off the Orkney Islands was compared to measurements from a nearby Waverider buoy. It was determined through spectral analysis that the model performed poorly when predicting low-frequency intermediate waves from the West.

Bertotti and Cavaleri [30] also stresses the importance of examining full two-dimensional spectra instead of just wave parameters (such as significant wave height, energy period, and mean wave direction). Analysis of the full spectrum can reveal complex trends and problems that are imperceptible in analysis of simple wave parameters. For example, looking at the directional spectra could uncover that the model is not correctly displaying multiple peaks within a spectrum. Bertotti and Cavaleri [30] also suggest that only looking at *one*-dimensional spectra (studying dependence only on frequency) is insufficient as a one-dimensional spectral analysis

would mask “different wave systems [that] may be present in the same frequency range” [30] as well as the effects of directionality which are especially important in stormy seas. While the problem areas of our model are specific to our study, the methodology can be used generally to uncover numerous other areas of weaknesses within models. For example, the procedure in this paper can be used to separate problems due to swell waves from those due to wind waves, to reveal missing peaks (by looking at error within every spectral bin), or to expose problems with predictions of extreme values (large errors can be easily seen in one-dimensional spectral graphs, such as Figures 4 and 6).

There are several sources of uncertainty in this study. As mentioned in section 2.1, the ranges of frequencies differ between the model and the buoy. Since most of the problems occur in low frequencies, the fact that the buoy starts from 0.0225 Hz and the model starts from 0.055 Hz may be the cause of some of our problems. Also, there is uncertainty in the directionality due to the directional spreading function we had to apply to the buoy (section 2.1). It would have been interesting to see if an alternative spreading function, such as $\cos 2s$, may have better represented the spectra. Another weakness in the methodology is that it does not show differences of spectral fit throughout the year and according to season.

As previously mentioned in the introduction, none of the wave resource assessments reviewed in Part 1 of this study [4, 5, 31-38] compare two-dimensional spectra within their verifications. In fact, the detail within this paper is more similar to validations done by wave modellers. Many of these types of studies [1, 7, 39, 12, 11] look at frequency and/or directional spectra for particular time records to examine model performance in more detail. A couple of these studies look at agreement for more than just a few particular records; Wyatt et al. [8] compare frequency and directional spectra from multiple models and a buoy side-by-side over a short time period. Janssen [40] looks at spectral bias (similar to what we did in Figure 6) and how it changes over 8 years.

The aim of this study was simply to demonstrate the detail needed within a verification section, and not to perform a full resource assessment for the coast of Island of Mainland, Orkney Islands, and hence it ends here. If it were a full resource assessment, the fundamental next step would be to nest a coastal model such as SWAN into the global model WAM. Shallow water physics will likely explain some or all of the errors and result in a better model performance. Zijlema [41] shows an unstructured-grid example for SWAN, showing a good performance for coastal waters. Wornom et al. [42] specifically compare SWAN and WAM results for a nearshore location, concluding that nesting SWAN into WAM increases the accuracy by up to 31%.

To conclude, the importance of each step in this study is emphasized. The methodology described in Part 1 led to the investigations done in Part 2, and the process outlined in Part 2 enabled the postulation of the educated hypotheses necessary for the next steps. Each step added to our understanding of the fit of the model at the location of interest and the reliability of the data.

Acknowledgements
This work was supported by the EU FP7 project, “MARINA Platform” (Grant agreement number 241402). The authors would like to thank the Atmospheric Modeling & Weather Forecasting Group at NKUA, especially Ms. Christina Kalogeri, for provision of data and advice on the analysis. The European Marine Energy Centre (EMEC) are gratefully acknowledged for provision of the Waverider buoy data.

References

[1] The WAMDI Group. The WAM model—a third generation wave prediction model. Journal of Physical Oceanography 1988;18:1775-1810.

[2] Janssen P, “Chapter 3 ECMWF wave modeling and satellite altimeter wave data,”in in *Satellites, oceanograghy and society*, vol. Volume 63, D. H. B. T.-E. O. Series, Ed. Elsevier, 2000, pp. 35–56.

[3] J. R. Bidlot and P. Janssen, “Unresolved bathymetry, neutral winds, and new stress tables in WAM,” 2003.

[4] Liberti L, Carillo A, Sannino G. Wave energy resource assessment in the Mediterranean, the Italian perspective. Renewable Energy 2013;50:938-949.

[5] van Nieuwkoop JCC, Smith HCM, Smith GH, Johanning L. Wave resource assessment along the Cornish coast (UK) from a 23-year hindcast dataset validated against buoy measurements. Renewable Energy 2013;58:1-14.

[6] Bidlot JR, Holmes DJ, Wittmann PA, Lalbeharry R, Chen HS. Intercomparison of the performance of operational ocean wave forecasting systems with buoy data. Weather and Forecasting 2002;17:287-310.

[7] Li JG, Holt M. Validation of a regional wave model with envisat and buoy observations. In: Proceedings of the Envisat Symposium; 2007. Montreux, Switzerland.

[8] Wyatt LR, Green JJ, Gurgel KW, Borge N, Reichert K, Hessner K, Günther H, Rosenthal W, Saetra O, Reistad M. Validation and intercomparisons of wave measurements and models during the EuroROSE experiments. Coastal Engineering 2003;48:1-28.

[9] Cavaleri L, Bertotti L, Lionello P. Shallow water application of the third-generation WAM wave model. Journal of Geophysical Research 1989;94:8111-8124.

[10] Janssen PAEM, Abdalla S, Hersbach H, Bidlot JR. Error estimation of buoy, satellite, and model wave height data. Journal of Atmospheric and Oceanic Technology 2007;24:1665-1676.

[11] Ris RC, Holthuijsen LH, Booij N. A third-generation wave model for coastal regions: 2. verification. Journal of Geophysical Research 1999;104:7667-7681.

[12] The WISE Group. Wave modelling – the state of the art. Progress in Oceanography 2007;75:603-674.

[13] Krogstad HE, Wolf J, Thompson SP, Wyatt LR. Methods for intercomparison of wave measurements. Coastal Engineering 1999;37:235-257.

[14] Mackay EBL, Bahaj AS, Challenor PG. Uncertainty in wave energy resource assessment. Part 1: Historic data. Renewable Energy 2010;35:1792-1808.

[15] U.S. Army Engineer Waterways Experiment Station, Coastal Engineering Research Center. Coastal engineering technical note: Directional wave spectra using normal spreading function. Available at: http://chl.erdc.usace.army.mil/library/publications/chetn/pdf/cetn-i-6.pdf; 1985 [accessed 19.8.2013].

[16] Janssen PAEM. The interaction of ocean waves and wind. Cambridge University Press; 2004.

[17] WAMDIG, The WAM-Development and Implementation Group: Hasselmann S, Hasselmann K, Bauer E, Bertotti L, Cardone CV, Ewing JA, Greenwood JA, Guillaume A, Janssen PAEM, Komen GJ, Lionello P, Reistad M, Zambresky L. The WAM model - a third generation ocean wave prediction model. Journal of Physical Oceanography 1988;18:1775-1810.

[18] Komen G, Cavaleri L, Donelan M, Hasselmann K, Hasselmann S, Janssen PAEM. Dynamics and modelling of ocean waves. Cambridge University Press; 1994.

[19] Bidlot J, Janssen P, Abdalla S, Hersbah H. A revised formulation of the ocean wave dissipation and its model impact. ECMWF Tech Memo. Reading, United Kingdom; 2007; 509.

[20] Janssen PAEM, Onorato M. The Intermediate Water Depth Limit of the Zakharov Equation and Consequences for Wave Prediction. J.Phys.Oceanogr. 2007;37:2389-2400.

[21] Kallos G, 1997: The Regional weather forecasting system SKIRON. Proceedings of the Symposium on Regional Weather Prediction on Parallel Computer Environments, 15-17 October 1997, Athens, Greece.

[22] Spyrou C, Mitsakou C, Kallos G, Louka V, Vlastou G. An improved limited area model for describing the dust cycle in the atmosphere, Journal of geophysical research 2010, 115, D17211, doi: 10.1029/2009JD013682.

[23] Datawell. Datawell File Formats. Available at: http://www.datawell.nl/Portals/0/Documents/TechnicalNotes/datawell_technicalnote_fileformats_2013-03-14.pdf; 2013 [accessed 19.8.2013].

[24] Tucker, MJ. Recommended standard for wave data sampling and near-real-time processing. Ocean Engineering 1993;20:459-474.

[25] DIWASP, a directional wave spectra toolbox for MATLAB: User Manual. Research Report WP-1601-DJ (V1.4), Centre for Water Research, University of Western Australia. Available at: http://www.metocean.co.nz/wp-content/uploads/2011/09/DIWASP_manual.pdf [accessed 19.8.2013].

[26] Lemon J et al. Package 'plotrix' Available at: http://cran.r-project.org/web/packages/plotrix/plotrix.pdf; 2013 [accessed 19.8.2013].

[27] Akima H, Gebhardt A, Petzoldt T, Maechler M. Package 'akima' Available at: http://cran.r-project.org/web/packages/akima/akima.pdf; 2013 [accessed 19.8.2013].

[28] Furrer R, Nychka D, Sain S. Package 'fields' Available at: http://cran.r-project.org/web/packages/fields/fields.pdf; 2013 [accessed 19.8.2013].

[29] Rahman M. Water Waves: Relating Modern Theory to Advanced Engineering Practice. Oxford: Clarendon Press; 1995.

[30] Bertotti L, Cavaleri L. Modelling waves at Orkney coastal locations. Journal of Marine Systems 2012;96-97:116-121.

[31] Mørk G, Barstow S, Kabuth A, Pontes MT. Assessing the global wave energy potential. Proceedings of the 29th International Conference on Ocean, Offshore Mechanics and Arctic Engineering 2010.

[32] Arinaga RA, Cheung KF. Atlas of global wave energy from 10 years of reanalysis and hindcast data. Renewable Energy 2012;39:49-64.

[33] ESBI Engineering & Facility Management Ltd. Accessible Wave Energy Resource Atlas: Ireland: 2005. Available at: http://www.marine.ie/NR/rdonlyres/90ECB08B-A746-4247-A277-7F9231BF2ED2/0/waveatlas.pdf; 2005 [accessed 19.8.2013].

[34] ABP Marine Environmental Research Ltd. Atlas of UK Marine Renewable Energy Resources: Technical Report. Available at: http://www.renewables-atlas.info/downloads/documents/R1432_Final_15May08.pdf; 2008 [accessed 19.8.2013].

[35] Vengatesan V, Davey T, Girard F, Smith H, Smith G, Cavaleri L, Bertotti L, Lawrence J. Equitable Testing and Evaluation of Marine Energy Extraction Devices in terms of Performance, Cost and Environmental Impact (EquiMar): Deliverable D2.3

Application of Numerical Models. Available at: https://www.wiki.ed.ac.uk/display/EquiMarwiki/EquiMar;jsessionid=E74D286B9C35837A252BD33B4836D848; 2010 [accessed 19.8.2013].

[36] Iglesias G, Carballo R. Wave resource in El Hierro—an island towards energy self-sufficiency. Renewable Energy 2011;36:689-698.

[37] Lenee-Bluhm P, Paasch R, Özkan-Haller HT. Characterizing the wave energy resource of the US Pacific Northwest. Renewable Energy 2011;36:2106-2119.

[38] Stopa JE, Filipot JF, Li N, Cheung KF, Chen YL, Vega L. Wave energy resources along the Hawaiian Island chain. Renewable Energy 2013;55:305-321.

[39] Portilla J, Ocampo-Torres FJ, Monbaliu J. Spectral partitioning and identification of wind sea and swell. Journal of Atmospheric and Oceanic Technology 2009;26:107-122.

[40] Janssen PAEM. Progress in ocean wave forecasting. Journal of Computational Physics 2008;227:3572-3594.

[41] Zijlema M. Computation of wind-wave spectra in coastal waters with SWAN on unstructured grids. Coastal Engineering 2010;57:267-277.

[42] Wornom SF, Welsh DJS, Bedford KW. On coupling the SWAN and WAM wave models for accurate nearshore wave predictions. Coastal Engineering Journal 2001;43:161.